

# Discriminative strain and temperature measurement using Brillouin scattering and fluorescence in erbium-doped optical fiber

Mingjie Ding,<sup>1,2</sup> Yosuke Mizuno,<sup>1,\*</sup> and Kentaro Nakamura<sup>1</sup>

<sup>1</sup>Precision and Intelligence Laboratory, Tokyo Institute of Technology, Yokohama 226-8503, Japan

<sup>2</sup>School of Electrical Engineering and Telecommunications, University of New South Wales, Sydney, New South Wales 2052, Australia

\*ymizuno@sonic.pi.titech.ac.jp

**Abstract:** We develop a novel discriminative sensing technique of strain and temperature using Brillouin scattering and fluorescence in an erbium-doped fiber (EDF). First, we show that the fluorescence intensity ratio (FIR), the ratio of the fluorescence intensities at two different wavelengths (1530 nm and 1565 nm in this experiment), is linearly dependent on temperature (with a coefficient of  $5.6 \times 10^{-4}$  /°C) but almost independent of strain. Then, by combined use of the FIR and the Brillouin frequency shift in an EDF, we experimentally demonstrate discriminative measurements of strain and temperature with four different sets of strain and temperature changes.

©2014 Optical Society of America

**OCIS codes:** (120.0280) Remote sensing and sensors; (280.4788) Optical sensing and sensors; (290.5830) Scattering, Brillouin.

---

## References and links

1. T. Horiguchi and M. Tateda, "BOTDA – nondestructive measurement of single-mode optical fiber attenuation characteristics using Brillouin interaction: theory," *J. Lightwave Technol.* **7**(8), 1170–1176 (1989).
2. T. Kurashima, T. Horiguchi, H. Izumita, S. Furukawa, and Y. Koyama, "Brillouin optical-fiber time domain reflectometry," *IEICE Trans. Commun.* **E76-B**, 382–390 (1993).
3. D. Garus, K. Krebber, F. Schliep, and T. Gogolla, "Distributed sensing technique based on Brillouin optical-fiber frequency-domain analysis," *Opt. Lett.* **21**(17), 1402–1404 (1996).
4. K. Hotate and T. Hasegawa, "Measurement of Brillouin gain spectrum distribution along an optical fiber using a correlation-based technique – proposal, experiment and simulation –, " *IEICE Trans. Commun.* **E83-C**, 405–412 (2000).
5. Y. Mizuno, W. Zou, Z. He, and K. Hotate, "Proposal of Brillouin optical correlation-domain reflectometry (BOCDR)," *Opt. Express* **16**(16), 12148–12153 (2008).
6. C. C. Lee, P. W. Chiang, and S. Chi, "Utilization of a dispersion-shifted fiber for simultaneous measurement of distributed strain and temperature through Brillouin frequency shift," *J. Lightwave Technol.* **13**, 1094–1096 (2001).
7. W. Zou, Z. He, M. Kishi, and K. Hotate, "Stimulated Brillouin scattering and its dependences on strain and temperature in a high-delta optical fiber with F-doped depressed inner cladding," *Opt. Lett.* **32**(6), 600–602 (2007).
8. T. R. Parker, M. Farhadiroushan, V. A. Handerek, and A. J. Rogers, "Temperature and strain dependence of the power level and frequency of spontaneous Brillouin scattering in optical fibers," *Opt. Lett.* **22**(11), 787–789 (1997).
9. X. Bao, Q. Yu, and L. Chen, "Simultaneous strain and temperature measurements with polarization-maintaining fibers and their error analysis by use of a distributed Brillouin loss system," *Opt. Lett.* **29**(12), 1342–1344 (2004).
10. W. Zou, Z. He, and K. Hotate, "Complete discrimination of strain and temperature using Brillouin frequency shift and birefringence in a polarization-maintaining fiber," *Opt. Express* **17**(3), 1248–1255 (2009).
11. W. Zou, Z. He, K. Y. Song, and K. Hotate, "Correlation-based distributed measurement of a dynamic grating spectrum generated in stimulated Brillouin scattering in a polarization-maintaining optical fiber," *Opt. Lett.* **34**(7), 1126–1128 (2009).
12. M. Ding, N. Hayashi, Y. Mizuno, and K. Nakamura, "Brillouin gain spectrum dependences on temperature and strain in erbium-doped optical fibers with different erbium concentrations," *Appl. Phys. Lett.* **102**(19), 191906 (2013).

13. T. Horiguchi, T. Kurashima, and M. Tateda, "Tensile strain dependence of Brillouin frequency shift in silica optical fibers," *IEEE Photon. Technol. Lett.* **1**(5), 107–108 (1989).
14. T. Kurashima, M. Tateda, and M. Tateda, "Thermal effects on the Brillouin frequency shift in jacketed optical silica fibers," *Appl. Opt.* **29**(15), 2219–2222 (1990).
15. L. Zou, X. Bao, S. Afshar V, and L. Chen, "Dependence of the Brillouin frequency shift on strain and temperature in a photonic crystal fiber," *Opt. Lett.* **29**(13), 1485–1487 (2004).
16. Y. Mizuno and K. Nakamura, "Potential of Brillouin scattering in polymer optical fiber for strain-insensitive high-accuracy temperature sensing," *Opt. Lett.* **35**(23), 3985–3987 (2010).
17. Y. Mizuno, N. Hayashi, and K. Nakamura, "Dependences of Brillouin frequency shift on strain and temperature in optical fibers doped with rare-earth ions," *J. Appl. Phys.* **112**(4), 043109 (2012).
18. E. Desurvire, *Erbium-Doped Fiber Amplifiers* (John Wiley, 1994).
19. H. Kusama, O. J. Sovers, and T. Yoshioka, "Line shift method for phosphor temperature measurements," *Jpn. J. Appl. Phys.* **15**(12), 2349–2358 (1976).
20. Y. Imai and T. Hokazono, "Fluorescence-based temperature sensing using erbium-doped optical fibers with 1.48  $\mu\text{m}$  pumping," *Opt. Rev.* **4**(1), 117–120 (1997).
21. S. F. Collins, G. W. Baxter, S. A. Wade, T. Sun, K. T. V. Grattan, Z. Y. Zhang, and A. W. Palmer, "Comparison of fluorescence-based temperature sensor schemes: theoretical analysis and experimental validation," *J. Appl. Phys.* **84**(9), 4649–4654 (1998).
22. S. A. Wade, S. F. Collins, and G. W. Baxter, "Fluorescence intensity ratio technique for optical fiber point temperature sensing," *J. Appl. Phys.* **94**(8), 4743–4756 (2003).
23. V. K. Rai and S. B. Rai, "Temperature sensing behavior of the stark sublevels," *Spectrochim. Acta Mol. Biomol. Spectrosc.* **68**(5), 1406–1409 (2007).
24. M. Ding, N. Hayashi, Y. Mizuno, and K. Nakamura, "Brillouin signal amplification in pumped erbium-doped optical fiber," *IEICE Electron. Express* **11**(18), 20140627 (2014).

## 1. Introduction

As a promising technology for structural health monitoring, fiber-optic distributed strain and temperature sensing based on Brillouin scattering has been extensively studied for several decades [1–5], and various measurement techniques in time- [1,2], frequency- [3], and correlation-domains [4,5] have been developed. Their basic operating principle lies in the linear dependence of the Brillouin frequency shift (BFS) on strain and temperature. However, only by measuring the BFS, response to strain cannot be separated from that to temperature. Thus, the discriminative measurement of strain and temperature has been one of the main issues to be tackled in fiber-optic Brillouin sensing community.

One solution is to use two optical fibers: one is embedded into the structure to detect the total effects of strain and temperature, while the other is kept loose (or packed in a thermal insulation jacket) so that it can feel temperature (or strain) only; then these two parameters can be numerically calculated. However, using two optical fibers increases the failure risk and installation difficulty in practical implementation. Some research groups [6,7] have tried to utilize multiple acoustic resonance peaks at different orders of Brillouin gain spectrum (BGS) in a single specially-designed optical fiber, but the discrimination accuracy was not sufficient because all the acoustic resonance frequencies show similar behaviors in their dependences on strain and temperature. Another method is to make use of the peak amplitude (or bandwidth) and BFS in the BGS simultaneously [8,9], but the discrimination accuracy was not sufficient either chiefly because of the low signal-to-noise ratio in the distributed measurement of the peak amplitude (or bandwidth). Zou et al. [10,11] have demonstrated completely discriminative distributed strain/temperature sensing exploiting a so-called Brillouin dynamic grating in a polarization-maintaining (PM) fiber. Although the strain and temperature discrimination accuracies were as good as 3  $\mu\epsilon$  and 0.08  $^{\circ}\text{C}$ , respectively, its experimental setup was rather complicated, containing many expensive PM devices.

In this work, we show in a proof-of-concept demonstration that a discriminative strain and temperature measurement can be performed using the BFS and the fluorescence intensity ratio (FIR) in an erbium-doped fiber (EDF). The FIR, determined by the fluorescence intensities at two different wavelengths (1530 nm and 1565 nm in this experiment), shows a linear temperature dependence with a slope of  $5.6 \times 10^{-4} / ^{\circ}\text{C}$ , but scarcely depend on strain. In combination with the previously reported results on the BFS dependences on strain and

temperature in EDFs [12], we experimentally demonstrate a discriminative measurement of strain and temperature in four cases, where estimated values agree well with actual values.

## 2. Principle

Pump light injected into an optical fiber interacts with acoustic phonons, and generates backscattered Stokes light. This phenomenon is known as spontaneous Brillouin scattering, and the Stokes light spectrum, referred to as the BGS, takes the shape of a Lorentzian function. The central frequency of the BGS shifts downward relative to that of the pump light by the amount called the BFS. At 1.55- $\mu\text{m}$  pumping wavelength, the BFS in glass fibers is approximately 11 GHz, which slightly varies depending on the fiber fabrication process and/or dopants. The BFS is generally dependent on applied strain and temperature in the fibers, and the BFS dependences have been investigated in various fibers, such as silica single-mode fibers (SMFs) [13,14], photonic crystal fibers [15], polymer optical fibers [16], and rare-earth-doped fibers [12,17]. In an EDF with 720-wtppm erbium concentration, the proportionality constants of the BFS dependences on strain and temperature at 1.55  $\mu\text{m}$  are reported to be 479 MHz/% and 0.87 MHz/ $^{\circ}\text{C}$ , respectively [12]. Thus, by measuring the BFS distribution along a fiber, the information on applied strain or temperature distribution can be obtained.

Fluorescence in an EDF occurs through the radiative transition of erbium ions between different energy levels; specifically, from  $^4I_{13/2}$  to  $^4I_{15/2}$  in 980-nm pumping configuration [18]. The fluorescence intensity is known to be dependent on temperature, but direct use of the intensity is not suitable for practical sensor applications because of the signal fluctuations influenced by external loss. One method of overcoming this problem is to make use of FIR, defined as the ratio of the fluorescence intensities at two close but different energy levels (or wavelengths), which is immune to the incident power and polarization state [19–23]. According to the theory [18,21], the FIR is proportional to  $\exp(-\Delta E/kT)$ , where  $\Delta E$  is an energy difference between the two energy levels,  $k$  is a Boltzmann constant, and  $T$  is absolute temperature. Thus, temperature information can be derived from FIR measurement.

Once BFS and FIR dependences on strain and temperature in an EDF are obtained, strain and temperature can be calculated by

$$\begin{bmatrix} \Delta\varepsilon \\ \Delta T \end{bmatrix} = \frac{1}{C_{BFS}^e \cdot C_{FIR}^T - C_{BFS}^T \cdot C_{FIR}^e} \begin{bmatrix} C_{FIR}^T & -C_{BFS}^T \\ -C_{FIR}^e & C_{BFS}^e \end{bmatrix} \begin{bmatrix} \Delta BFS \\ \Delta FIR \end{bmatrix}, \quad (1)$$

where  $\Delta\varepsilon$ : applied strain change,  $\Delta T$ : ambient temperature change,  $C_{BFS}^e$  ( $C_{BFS}^T$ ): strain (temperature) coefficient of BFS,  $C_{FIR}^e$  ( $C_{FIR}^T$ ): strain (temperature) coefficient of FIR,  $\Delta BFS$ : BFS change, and  $\Delta FIR$ : FIR change. As demonstrated later in this paper, the FIR in an EDF is almost independent of strain, i.e.,  $C_{FIR}^e \approx 0$ . Consequently, Eq. (1) becomes

$$\begin{bmatrix} \Delta\varepsilon \\ \Delta T \end{bmatrix} = \frac{1}{C_{BFS}^e \cdot C_{FIR}^T} \begin{bmatrix} C_{FIR}^T & -C_{BFS}^T \\ 0 & C_{BFS}^e \end{bmatrix} \begin{bmatrix} \Delta BFS \\ \Delta FIR \end{bmatrix}, \quad (2)$$

the simplicity of which is one of the advantages of this method.

## 3. Experiments

In the experiment, we used a 0.6-m-long EDF with an erbium concentration of 720 wtppm, a core refractive index of  $\sim 1.47$ , a mode-field diameter of 7.2  $\mu\text{m}$ , and a peak absorption at 1.53  $\mu\text{m}$  of 18 dB/m. Both ends of the EDF were spliced to 1-m-long silica SMFs by using a fusion splicer, where the splicing loss was suppressed to  $< 0.1$  dB by optimizing the arc duration. The EDF was placed on a heater and both ends (spliced parts) were fixed on moving stages so that strain and temperature might be independently and simultaneously applied. The experimental setup is depicted in Fig. 1. Two laser diodes (LDs) were used; one at 1550 nm

for exciting Brillouin scattering in an EDF, and the other at 980 nm for enhancing the Brillouin scattering power [24] as well as for exciting the fluorescence in the EDF. During the FIR measurement, the LD at 1550 nm was not operated. The Brillouin Stokes light was heterodyned with the reference light, converted into an electrical signal with a photo diode, and then observed as BGS with an electrical spectrum analyzer (see [24] for details). The fluorescence spectrum of the EDF was observed with an optical spectrum analyzer (OSA). The polarization states were optimized for all the measurements using polarization controllers.

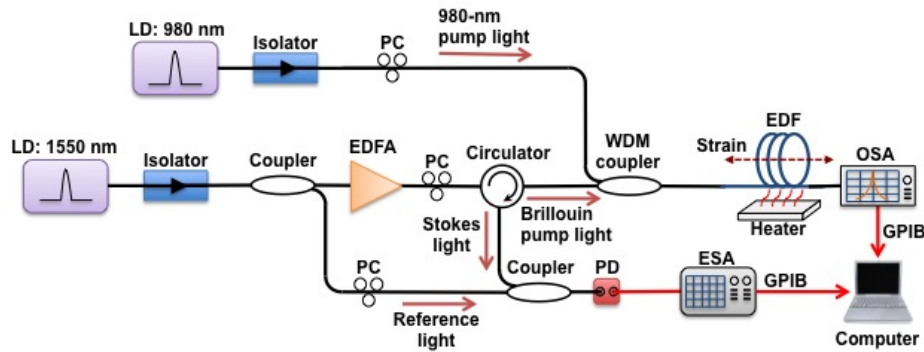


Fig. 1. Experimental setup. EDF(A): erbium-doped fiber (amplifier), ESA: electrical spectrum analyzer, GPIB: general-purpose interface bus, LD: laser diode, OSA: optical spectrum analyzer, PC: polarization controller, PD: photo diode, WDM: wavelength division multiplexing.

Figure 2 shows the measured temperature dependence of the fluorescence spectra in the EDF pumped at 980 nm. The power of the pump light was fixed at 26 dBm (maximal output of our LD; the pump power should be as high as possible to enhance the signal-to-noise ratio of the measurement). The temperature was increased from 30.0 to 100.0°C. A fluorescence peak was observed at around 1530 nm. In this experiment, we define the FIR as the ratio of the fluorescence intensity at 1565 nm to that at 1530 nm (note that the intensity ratio is equal to the power ratio). The magnified views of the fluorescence spectra at 1530 nm and 1565 nm are shown in the insets of Fig. 2. With increasing temperature, the optical power was decreased at 1530 nm and increased at 1565 nm. Using these data, we calculated the temperature dependence of the FIR, as shown in Fig. 3(a). In the temperature range from 30.0 to 100.0°C, the FIR was linearly dependent on ambient temperature with a proportionality constant  $C_{\text{FIR}}^T$  of  $5.6 \times 10^{-4} / ^\circ\text{C}$ . The strain dependence of the FIR was also measured as displayed in Fig. 3(b). The strain dependence coefficient was calculated to be  $6.8 \times 10^{-3} / \%$ , but unstable FIR values suggest that the strain dependence is negligibly small. Thus, even when strain and temperature changes are simultaneously applied to the EDF, temperature information can be separately obtained by FIR measurement results.

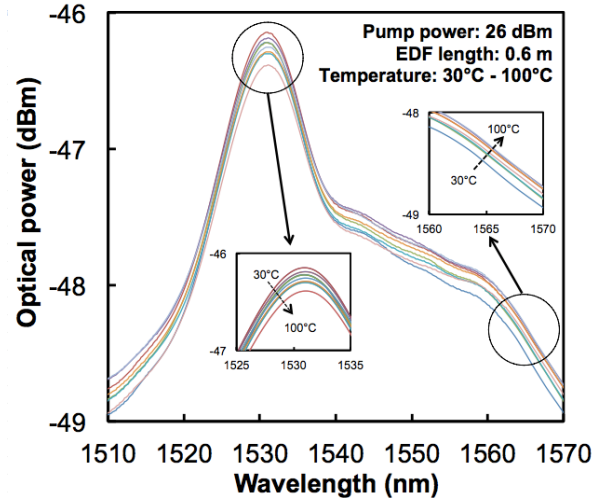


Fig. 2. Fluorescence spectra in EDF. The insets show the magnified views at around (a) 1530 nm and (b) 1565 nm.

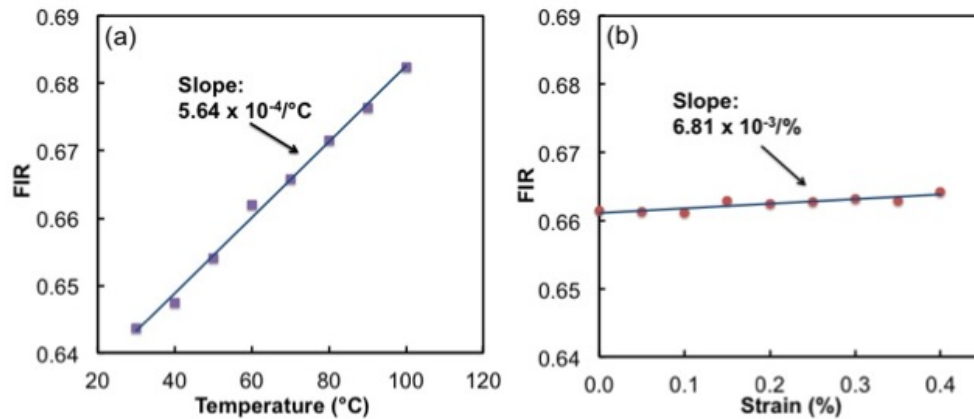


Fig. 3. FIR measured as a function of (a) temperature and (b) strain.

We then demonstrate discriminative sensing of strain and temperature in combination with Brillouin measurement in four cases. The power of the Brillouin pump light was fixed at 28 dBm. First, without applying a strain to the EDF, the ambient temperature was raised from 30.0 to 100.0°C (temperature change of 70.0°C). Correspondingly, the FIR increased from 0.641 to 0.681 (FIR change of 0.040), while the BFS change was 51.2 MHz (calculated using Lorentzian-fitted data), as observed in Fig. 4(a). By substituting these parameters along with  $C_{BFS}^c = 479$  MHz/% and  $C_{BFS}^T = 0.87$  MHz/°C [12] into Eq. (2), the strain and temperature changes were estimated to be 0.02% and 71.4°C, which are in good agreement with the actual values with measurement errors of 0.02% and 1.4°C, respectively. Then, a 0.40% strain was applied to the EDF while the temperature was kept at 30.0°C. The FIR decreased from 0.641 to 0.639 (−0.002 change), and the BFS change was 174.4 MHz (Fig. 4(b)). Using Eq. (2), the strain and temperature changes were estimated to be 0.37% and −3.8°C with measurement errors of −0.03% and −3.8°C, respectively. Finally, we performed discriminative sensing in two cases where strain and temperature changes were simultaneously applied. When the strain increased from 0.30 to 0.40% (0.10% change) and the temperature was raised from 40.0 to 90.0°C (50.0°C change), the FIR increased from 0.648 to 0.676 (0.028 change), whereas the BFS change was 88.0 MHz (Fig. 4(c)). Then the strain and temperature changes were

estimated to be 0.09% and 51.0°C with measurement errors of  $-0.01\%$  and  $1.0^\circ\text{C}$ , respectively. In the same way, when the strain increased from 0.05 to 0.45% (0.40% change) and the temperature was raised from 90.0 to  $100.0^\circ\text{C}$  (10.0°C change), the FIR increased from 0.677 to 0.682 (0.005 change), and the BFS change was 196.8 MHz (Fig. 4(d)), resulting in the strain and temperature changes of 0.39% and  $8.2^\circ\text{C}$  with measurement errors of  $-0.01\%$  and  $-1.8^\circ\text{C}$ , respectively. These discriminative measurement results are summarized in Table 1. Thus, discriminative measurability of this strain/temperature sensing technique was experimentally proved.

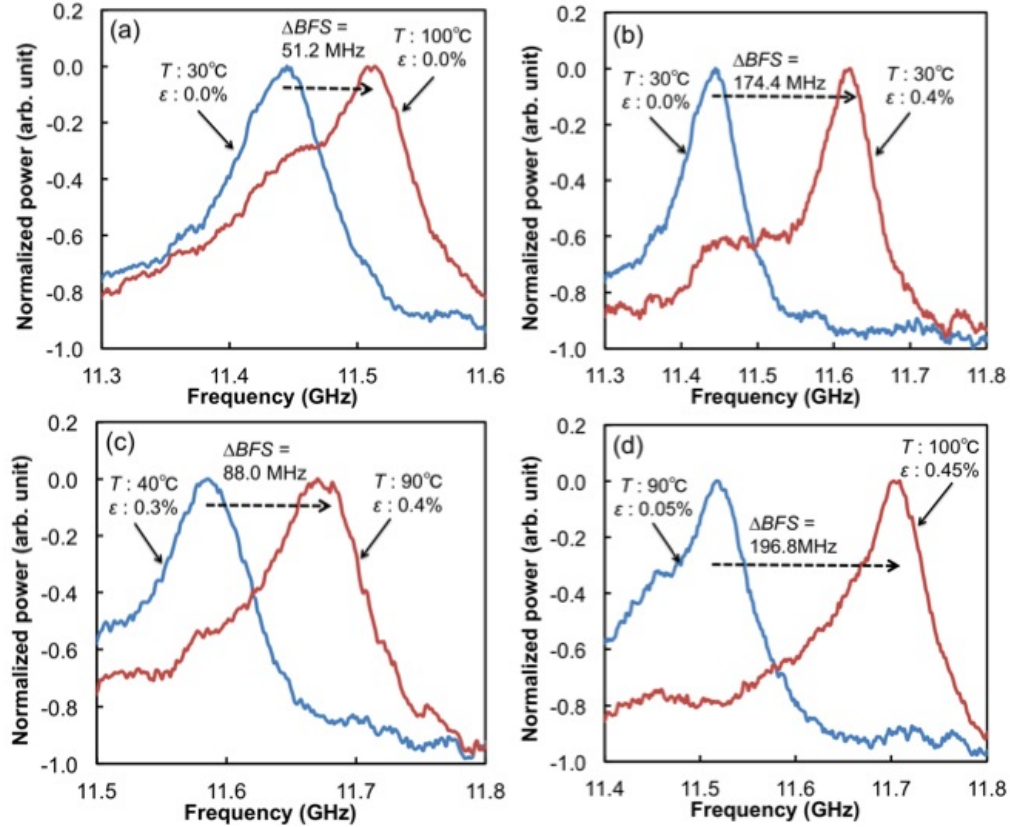


Fig. 4. (a)–(d) BGS shift in the EDF measured with four different sets of strain and temperature changes.

Table 1. Summary of discriminative measurement results.

| Actual values       |   | Estimated values    |   | Errors              |   |
|---------------------|---|---------------------|---|---------------------|---|
| $\Delta$ strain (%) | $\Delta$ temperature ( $^\circ\text{C}$ ) | $\Delta$ strain (%) | $\Delta$ temperature ( $^\circ\text{C}$ ) | $\Delta$ strain (%) | $\Delta$ temperature ( $^\circ\text{C}$ ) |
| 0.00                | 70.0                                      | 0.02                | 71.4                                      | 0.02                | 1.4                                       |
| 0.40                | 0.0                                       | 0.37                | $-3.8$                                    | $-0.03$             | $-3.8$                                    |
| 0.10                | 50.0                                      | 0.09                | 51.0                                      | $-0.01$             | 1.0                                       |
| 0.40                | 10.0                                      | 0.39                | 8.2                                       | $-0.01$             | $-1.8$                                    |

#### 4. Conclusion

We carried out a proof-of-concept demonstration of a discriminative strain/temperature measurement by simultaneous use of the FIR and BGS in an EDF for the first time to the best of our knowledge. The ratio of the fluorescence power at 1565 nm to that at 1530 nm was employed as the FIR in this experiment, which was found to be almost independent of applied strain. Strain and temperature changes estimated by this technique (e.g., 0.09% and 51.0°C) agreed well with the practical values (e.g., 0.10% and 50.0°C). The measurement time is at present not sufficiently short because of the internal scanning function of the OSA, which might be replaced by optical filters and power meters.

The next important challenge is to render this scheme distributed, referring to some techniques proposed to perform distributed Brillouin measurement [1–5]. We have to admit that the FIR distributed measurement cannot be achieved by a simple extension of conventional Brillouin techniques (using backscattered light) because of the following two reasons: (1) the FIR is measured using an OSA with a relatively low sampling rate, and (2) the FIR is measured for transmitted light. To resolve (1), we should acquire the FIR data with a high sampling rate without using an OSA. One implementation would be FIR detection with an oscilloscope after frequency downshift based on optical heterodyne and filtering. To resolve (2), the FIR measurement using not transmitted but reflected light should be explored. The current results presented in this paper, however, indicates that, in a special case where the EDF is uniformly heated (or cooled), strain distribution can be properly discriminated from the temperature information. Thus, we believe that our method is technologically attractive in implementing fiber-optic discriminative strain/temperature sensing systems in future.

#### Acknowledgments

We are indebted to Fujikura Ltd., Japan, for providing us with the EDF samples. We also appreciate Neisei Hayashi and Xinhua Guo, Tokyo Institute of Technology, Japan, for their experimental assistance and useful advice. This work was partially supported by Grants-in-Aid for Young Scientists (A) (no. 25709032) and for Challenging Exploratory Research (no. 26630180) from the Japan Society for the Promotion of Science (JSPS) and by research grants from the General Sekiyu Foundation, the Iwatani Naoji Foundation, and the SCAT Foundation.